

## Superradiant parametric x-ray emission

I. D. Feranchuk<sup>1,2,\*</sup>, N. Q. San<sup>3</sup>, and O. D. Skoromnik<sup>3,†</sup>

<sup>1</sup>*Atomicus GmbH, Schoemperlen Street 12a, 76185 Karlsruhe, Germany*

<sup>2</sup>*Belarusian State University, 4 Nezalezhnasty Avenue, 220030, Minsk, Belarus*

<sup>3</sup>*Department of Physics, Faculty of Electricity and Electronics,  
Nha Trang University, Nha Trang 57105, Vietnam*



(Received 19 June 2022; accepted 4 November 2022; published 23 December 2022)

We compute a spectrum of parametric x-ray radiation inside a crystal from a bunch of electrons, which is periodically modulated in density. We consider that the bunch of electrons is exiting from an x-ray free-electron laser (XFEL) channel. We demonstrate that in the case of a resonance between the frequency of parametric x-ray radiation and a frequency of modulation of an electron bunch, the sequence of strong quasimonochromatic x-ray pulses is formed—superradiant parametric x-ray emission (SPXE) with frequencies that are multiples of the modulation frequency. The number of photons in the pulse of SPXE in the case of extremely asymmetric diffraction is comparable with the photon number in the pulse of an XFEL. Moreover, the SPXE is directed under the large angle to the electron velocity and every harmonic in the spectrum is emitted under its own angle.

DOI: [10.1103/PhysRevAccelBeams.25.120702](https://doi.org/10.1103/PhysRevAccelBeams.25.120702)

### I. INTRODUCTION

Parametric x-ray radiation (PXR) is a well-known mechanism of radiation from charged particles propagating in a periodic medium [1–8]. Its qualitative properties are the emission of quasimonochromatic x-ray beams under the large angle to the electron velocity and the possibility to continuously tune the frequency of the radiation by simply rotating a crystal. As was first demonstrated in the work [9], when the electron density in the bunch reaches a critical value, the parametric beam instability can arise in analogy with the self-amplified spontaneous emission (SASE) in the undulator of an XFEL. This process leads to a spatial modulation of an electron beam and the generation of a coherent x-ray radiation under the scale of the crystal length, which is much smaller than the typical XFEL undulator lengths. However, under the currently experimentally accessible electron-beams densities, the length under which the parametric instability can be achieved is substantially larger than the x-ray absorption length in the crystal. Therefore, when an electron beam initially does not contain any modulation, it is almost impossible to realize the SASE mechanism inside a crystal.

Before discussing the superradiant parametric x-ray emission (SPXE), let us briefly revise how the undulator is used in the XFEL case [10]. On one hand, due to the SASE mechanism, the electron bunch, whose density was initially uniformly distributed, is transformed into a sequence of minibunches that leads to the spatial modulation of the electron density with the period  $d_0$ . This period is directly defined by the period of the undulator and defines the typical size of the minibunch. For the typical parameters of an XFEL, the size of the minibunch  $d_0 \approx 10^{-8}$  cm. Therefore, for the total bunch length  $L_b \approx 10^{-4}$  cm, the total number of minibunches  $K \approx 10^4 \gg 1$ . Later when the bunch propagates inside the undulator, coherent radiation is formed (superradiant emission [10]) with the frequency  $\omega_0 = 2\pi/d_0$  [11] and with the intensity proportional to the square of the number of electrons in the bunch. The coherent radiation is propagated in a small cone along the electron velocity. The coincidence (resonance) between the modulation frequency of the bunch and the frequency of the emitted photons happens automatically since the beam modulation and the emission frequency are determined by the same undulator radiation mechanism.

We also mention here that the secondary use of a modulated beam from an XFEL was analyzed in the work of the backward Compton scattering [12] and prebunched beam for XFEL [13].

Now let us consider the SPXE case when we suppose that an electron beam becomes modulated in density inside the undulator and in the end enters the crystalline target, where the PXR is generated with the frequency  $\omega_B$

\*Corresponding author.  
iferanchuk@gmail.com

†olegskor@gmail.com

Published by the American Physical Society under the terms of the [Creative Commons Attribution 4.0 International license](https://creativecommons.org/licenses/by/4.0/). Further distribution of this work must maintain attribution to the author(s) and the published article's title, journal citation, and DOI.

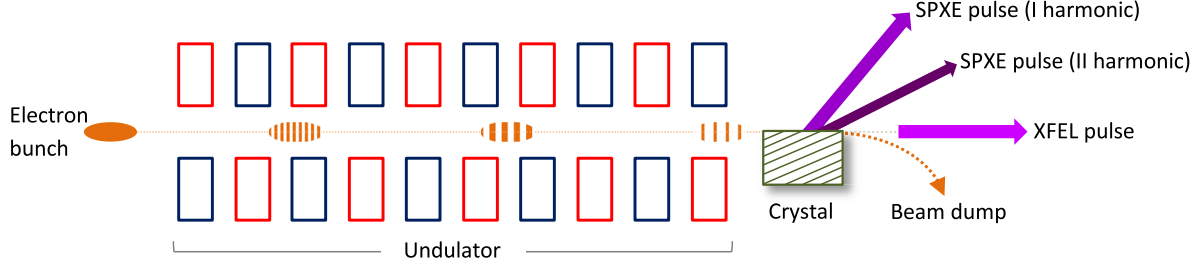


FIG. 1. Qualitative scheme of the processes which lead to the generation of SPXE pulses in the XFEL channel.

dependent on the crystal structure and the angle  $\theta_B$  between the crystallographic planes and the electron velocity. As was recently demonstrated in the work [14], the highest intensity of PXR is reached when the electrons propagate in the grazing geometry, i.e., in a thin layer inside the crystal parallel to the crystal-vacuum interface and the x-ray photons are emitted under the large angle  $2\theta_B$  to the electron velocity (PXR-EAD). The angle  $\theta_B$  can be chosen in such a way that the resonant condition  $\omega_0 \approx \omega_B$  is fulfilled. As a result, in addition to the main XFEL pulse, a generation of SPXE will happen with the intensity also proportional to the square of the number of electrons in the bunch. According to Ref. [1], the spectral density of PXR photons emitted by a single electron can be larger than the corresponding density of the undulator radiation. Consequently, the number of SPXE photons can exceed the corresponding number of the XFEL ones. Besides, the SPXE photon pulse is directed under the large angle to the electron velocity, which enlarges the applicability of the XFEL by the creation of the additional exiting channels of x rays. Figure 1 presents the qualitative picture of processes that lead to the SPXE pulses in the XFEL channel.

It is important to notice that the bunch of electrons remains modulated while it moves within the electromagnetic field of the XFEL pulse. For this reason, the crystal should be located directly near the exit from the undulator. At the same time, a part of XFEL photons will be reflected from the crystallographic planes of the crystal in the same direction as SPXE. The relative number of such photons with respect to the number of SPXE photons is determined by the reflection coefficient. This coefficient can be estimated as the ratio of the angular width of the Darwin step [15] ( $\sim 10^{-5}$ ) to the angular width of the XFEL pulse ( $\sim 10^{-3}$ ).

In our work, we describe a generation mechanism of SPXE and theoretically study characteristics of this new type of coherent x-ray radiation pulse that is emitted at a large angle to the direction of the electron velocity. The intensity of this pulse is proportional to the square of the number of electrons in the bunch and its characteristics are comparable with the parameters of the main XFEL pulse, which is directed along the electron velocity. SPXE pulses can be used for the creation of additional windows for XFEL with analogous applications [12]. Moreover, the higher harmonics of SPXE can be used for the generation

of the pulses of harder x rays and they do not require changing the energy of the electron bunch.

The paper is organized as follows: In Sec. II, we provide a qualitative analysis of the process of the formation of SPXE within a kinematic approximation, which is applicable to thin crystals. In Sec. III, we employ a dynamical theory of diffraction and demonstrate that the intensity of SPXE reaches its maximum when the electron bunch propagates the crystal with a length larger than the extinction length.

## II. QUALITATIVE ANALYSIS

### A. Method of the equivalent photons

We start the analysis of SPXE from its qualitative estimation by means of a simple and effective method of the description of electromagnetic processes of relativistic charged particles interacting with the medium, namely the method of equivalent photons (pseudophotons, Weizsacker-Williams approximation) [16–18]. This approach is based on the observation that the self-field of a relativistic charged particle is equivalent in its characteristics to the beam of pseudophotons with a spectral-angular distribution  $n(\mathbf{k})$  and a narrow angular divergence  $\approx \gamma^{-1}$ , which is determined by the relativistic gamma factor of the particle  $\gamma = E/m$  [11]. As a result, the differential cross section  $d\sigma_{if}^e$  of a transition  $i \Rightarrow f$  between the initial  $i$  and final state  $f$  of a charged particle moving with a velocity  $\mathbf{v}$  and interacting with the medium is represented as

$$d\sigma_{if}^e = n(\mathbf{k}) d\sigma_{if}^{\text{ph}}(\omega, \mathbf{k}_\perp) d\omega d\mathbf{k}_\perp, \quad (1)$$

where  $d\sigma_{if}^{\text{ph}}$  is the cross section of the same transition for a photon with the frequency  $\omega$  and the wave vector  $\mathbf{k} = (\omega v/v, \mathbf{k}_\perp)$ .

In this framework, PXR can be considered a diffraction of a beam of pseudophotons on the crystallographic planes. The spectral-angular distribution  $n(\mathbf{k})$  of pseudophotons for a single charged particle is well known [16–18] and is given by a smooth function of the frequency of the pseudophotons. For relativistic particles, the wave vector  $\mathbf{k}$  of a pseudophoton can be approximated as  $\mathbf{k} \approx \mathbf{k}_0 = \omega v/v$  with  $|\mathbf{k}_\perp| \ll k_0$ . As a result, PXR peaks are determined by the frequencies  $\omega_B$  when the wave vector  $\mathbf{k}_0$

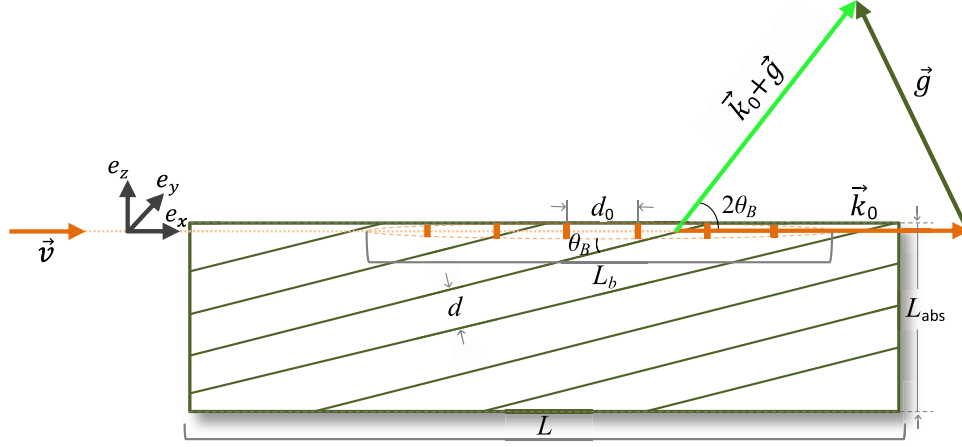


FIG. 2. Scheme of the photon generation in the case of PXR-EAD geometry.  $L_b \sim 10^{-4}$  cm is the modulated bunch length,  $L_{\text{abs}} \sim 10^{-2}$  cm is the radiation absorption length.

satisfies Bragg's condition. Consequently, the emitted photons are propagating in the directions of  $\mathbf{k}_0 + \mathbf{g}$ , where  $\mathbf{g}$  is one of the reciprocal lattice vectors of a crystal. As was demonstrated in Ref. [14], PXR will have the highest intensity when an electron moves in a crystal in a thin layer near the crystal surface, EAD geometry, and the emitted radiation can exit the crystal without absorption, see Fig. 2.

When we now consider an electron bunch consisting of  $N$  electrons uniformly spread in space, the total field will be given by an incoherent sum of fields from each electron. Therefore, the spectral-angular distribution of the pseudophotons is simply defined by the sum of contributions from each particle and equals  $Nn(\mathbf{k})$ .

However, if the electron beam was moving through the undulator due to the SASE mechanism, it became modulated. Accordingly, its density becomes a periodic function of the longitudinal coordinate with the period  $d_0$ . Consequently, this suggests that we might expect the coherent summation of individual fields from every electron. This results in the substantial modification of the total spectral distribution of pseudophotons in which we expect to see peaks with the amplitude proportional to the square of the number of particles in the beam. The frequencies of these spikes are harmonics of the frequency  $\omega_0$ . If the frequency of one of the peaks coincides with the frequency  $\omega_B$ , we should expect to see the resonant increase in the intensity of diffracted pseudophotons. This corresponds exactly to the SPXE pulse. The SPXE emission happens when Bragg's condition  $2k_0d \sin \theta_B = 2\pi$  for the reflection of pseudophotons from the crystallographic planes is simultaneously fulfilled with the coherence condition of the radiation from electrons of different minibunches  $k_0d_0 = 2\pi$ , that is,

$$2d \sin \theta_B = d_0 \quad (2)$$

see Fig. 2.

### B. Electromagnetic field of the electron bunch

Let us now investigate this process in more detail. In the range of frequencies, which are much smaller than the particle energy  $E$ , i.e.,  $\omega \ll E$  the spectrum of pseudophotons can be obtained via classical description [16]. The vector  $\mathbf{A}(\mathbf{r}, t)$  and scalar  $\varphi(\mathbf{r}, t)$  potentials from a beam of particles with charge  $e_0$  that move uniformly in vacuum are defined by the Maxwell equations

$$\square \mathbf{A} = -4\pi e_0 \sum_a^N \mathbf{v}_a \delta(\mathbf{r} - \mathbf{v}_a t - \mathbf{r}_a), \quad (3)$$

$$\square \varphi = -4\pi e_0 \sum_a^N \delta(\mathbf{r} - \mathbf{v}_a t - \mathbf{r}_a), \quad (4)$$

where  $\square$  is the d'Alembert operator  $\square = \partial^2/\partial t^2 - \nabla^2$ , the sum runs over all particles and each particle is located at the initial position  $\mathbf{r}_a$  and has the velocity  $\mathbf{v}_a$ .

The Fourier transform of Eqs. (3) and (4) allows one to find the potentials and calculate the electromagnetic fields.

$$\mathbf{E}(\mathbf{r}, t) = \sum_a^N \mathbf{E}_a(\mathbf{r}, t), \quad (5)$$

$$\mathbf{E}_a(\mathbf{r}, t) = -\frac{ie_0}{2\pi^2} \int d\mathbf{k} \frac{\mathbf{k} - \mathbf{v}_a(k\mathbf{v}_a)}{k^2 - (k\mathbf{v}_a)^2} e^{ik(\mathbf{r} - \mathbf{v}_a t - \mathbf{r}_a)}, \quad (6)$$

$$\mathbf{H}(\mathbf{r}, t) = \sum_a^N \mathbf{v}_a \times \mathbf{E}_a(\mathbf{r}, t). \quad (7)$$

Now we estimate the fields in Eq. (5). For this, we consider that the electron beam has a small angular divergence, such that the velocity of each particle can be presented as

$$\mathbf{v}_a = \mathbf{v} + \mathbf{v}'_a, \quad v'_a \ll v, \quad (8)$$

$$1 - v^2 = \frac{m^2}{E^2} \equiv \gamma^{-2} \ll 1. \quad (9)$$

We direct the  $x$  axis along the mean velocity  $\mathbf{v}$  of the bunch and suppose that the particle angular divergence is small with respect to this axis, i.e.,  $\theta_a < \gamma^{-1}$ , where the angle  $\theta_a$  defines this angular divergence. The fluctuations of the absolute value of the velocity are related to the nonmonochromaticity  $\Delta E$  of the beam  $|\mathbf{v}_a - \mathbf{v}| \approx \gamma^{-2} \Delta E/E \ll \gamma^{-2}$ . Taking this into account, we can represent the components of the fluctuation vector  $\mathbf{v}'_a$  of the particle velocity with the accuracy up to  $\gamma^{-2}$  as

$$\mathbf{v}'_a = \boldsymbol{\theta}_a - \frac{\theta_a^2}{2} \mathbf{e}_x, \quad \theta_a^2 = \theta_{az}^2 + \theta_{ay}^2, \quad (10)$$

$$\boldsymbol{\theta}_a = \theta_{az} \mathbf{e}_z + \theta_{ay} \mathbf{e}_y, \quad (11)$$

where  $\mathbf{e}_x$ ,  $\mathbf{e}_y$ ,  $\mathbf{e}_z$  are the unit vectors (see Fig. 2).

In this approximation, the denominator of the field amplitude in Eq. (6) equals to

$$k_x^2 \gamma^{-2} + (\mathbf{k}_\perp - k_x \boldsymbol{\theta}_a)^2 \quad (12)$$

and demonstrates that the main contribution to the field amplitude comes from the values

$$\theta_a \simeq \frac{k_\perp}{k_x} \simeq \gamma^{-1}. \quad (13)$$

For these angles, the field to an accuracy  $\gamma^{-1}$  becomes transverse since  $|E_x| \simeq \gamma^{-1} |E_\perp|$  and reads

$$\mathbf{E}_\perp(\mathbf{r}, t) = \sum_a^N \mathbf{E}_{a\perp}(\mathbf{r}, t), \quad (14)$$

$$\mathbf{E}_{a\perp}(\mathbf{r}, t) = -\frac{ie_0}{2\pi^2} \int d\mathbf{k} \frac{(\mathbf{k}_\perp - \boldsymbol{\theta}_a k_x) e^{ik(r - v_a t - r_a)}}{k_x^2 \gamma^{-2} + (\mathbf{k}_\perp - k_x \boldsymbol{\theta}_a)^2},$$

$$\mathbf{H}(\mathbf{r}, t) = \mathbf{v} \times \mathbf{E}_\perp(\mathbf{r}, t). \quad (15)$$

### C. Spectral density of the equivalent photons

The projection of the energy flux of the electromagnetic field on the  $x$  axis is determined by the following expression [16]:

$$\begin{aligned} \Pi &= \frac{1}{4\pi} \int_{-\infty}^{\infty} dz dy dt [\mathbf{E}\mathbf{H}]_x = \int_{-\infty}^{\infty} dx dy dt |\mathbf{E}_\perp|^2 \\ &\simeq \frac{e_0^2}{2\pi^2 v} \sum_a \sum_b \int d\mathbf{k} \frac{(\mathbf{k}_\perp - \boldsymbol{\theta}_a k_x)(\mathbf{k}_\perp - \boldsymbol{\theta}_b k_x) e^{ik(r_b - r_a)} e^{ixk(v'_a - v'_b)}}{(k_x^2 \gamma^{-2} + (\mathbf{k}_\perp - k_x \boldsymbol{\theta}_a)^2)(k_x^2 \gamma^{-2} + (\mathbf{k}_\perp - k_x \boldsymbol{\theta}_b)^2)}, \end{aligned} \quad (16)$$

which can be split into the sum of two parts

$$\Pi = \Pi_{\text{sp}} + \Pi_{\text{coh}}. \quad (17)$$

The incoherent (spontaneous) flux  $\Pi_{\text{sp}}$  is given by the part of the sum when the summation indices coincide, i.e.,  $a = b$ . After integration of this part over the variable  $(\mathbf{k}_\perp - \boldsymbol{\theta}_a k_x) \Rightarrow \mathbf{k}_\perp$ , the standard expression of the spectral density of pseudophotons for the homogeneous electron beam is obtained [16]

$$\begin{aligned} \Pi_{\text{sp}} &= \frac{e_0^2}{v 2\pi^2} N \int d\mathbf{k} \frac{k_\perp^2}{[k_x^2 \gamma^{-2} + \mathbf{k}_\perp^2]^2} = \int \omega n_{\text{sp}}(\omega) d\omega; \\ n_{\text{sp}}(\omega) &= N \frac{2e_0^2}{\pi\omega} \ln \frac{m\gamma}{\omega}, \end{aligned} \quad (18)$$

where  $|\mathbf{k}_\perp - \boldsymbol{\theta}_a| \leq \omega \gamma^{-1}$ ,  $N$  is the total number of electrons in the beam, and  $m$  is the mass of the electron.

The coherent part is given via the following expression:

$$\begin{aligned} \Pi_{\text{coh}} &= \frac{e_0^2}{2v\pi^2} \int d\mathbf{k} |\mathbf{F}(\mathbf{k})|^2, \\ \mathbf{F}(\mathbf{k}) &= \sum_a^N \frac{(\mathbf{k}_\perp - \boldsymbol{\theta}_a k_x)}{k_x^2 \gamma^{-2} + (\mathbf{k}_\perp - k_x \boldsymbol{\theta}_a)^2} e^{-ikr_a} e^{ixk v'_a}, \end{aligned} \quad (19)$$

where  $\mathbf{v}'_a = v \boldsymbol{\theta}_a$ . To compute the form factor  $\mathbf{F}(\mathbf{k})$  of the beam, we need to average the obtained expression over the distribution on the coordinates  $\mathbf{r}_a$  and the angles  $\boldsymbol{\theta}_a$  of the electrons in the beam. For this, we can employ the theory of the SASE mechanism of the XFEL, which yields the following expression for the desired distribution [10,19]:

$$\rho(\boldsymbol{\theta}) = \frac{1}{\pi\sigma_a^2} e^{-(\theta_z^2 + \theta_y^2)/\sigma_a^2}, \quad (20)$$

$$f(\mathbf{r}) = \frac{1}{\pi\sigma_b^2} e^{-(z^2 + y^2)/\sigma_b^2} \frac{1}{K} \sum_{l=0}^K \frac{1}{\sqrt{\pi}\sigma_c} e^{-(x - ld_0)^2/\sigma_c^2}. \quad (21)$$

Here the quantity  $\sigma_a$  defines the angular spread of the direction of the velocity,  $\sigma_b$  is the variance of the distribution over the transverse coordinates,  $d_0$  is the period of the oscillations of the modulated bunch of length  $L_b = Kd_0$ . It is also assumed that the parameter  $\sigma_c$  that defines the fluctuations of the period of the oscillations  $\sigma_c \ll d_0$  and the number of the minibunches  $K \gg 1$ . In addition, the distribution functions are normalized to unity.

Having this distribution, we can approximately substitute the summation over the discrete index  $a$  by the integration over the continuous variables

$$\sum_a^N \Rightarrow N \int dr d\theta f(\mathbf{r})\rho(\theta). \quad (22)$$

Let us now compute the integrals over the coordinates and angles. The coordinate part is simple and is given via the Fourier transform of the Gaussian integral

$$\begin{aligned} \int dr f(\mathbf{r})e^{-i\mathbf{k}\mathbf{r}} &= e^{-(k_z^2+k_y^2)\sigma_b^2/4} \frac{1}{K} \sum_{l=0}^K e^{-ik_x l d_0} e^{-k_x^2 \sigma_c^2/4} \\ &= e^{-(k_z^2+k_y^2)\sigma_b^2/4} \frac{1 - e^{iL_b k_x}}{K(1 - e^{id_0 k_x})} e^{-k_x^2 \sigma_c^2/4}. \end{aligned} \quad (23)$$

The averaging over the angular spreads is reduced to the following integral:

$$I = \int d\theta \frac{e^{-\theta^2/\sigma_a^2}}{k_x} \frac{1}{\pi\sigma_a^2} \frac{(\theta_k - \theta) e^{ixk_x v \theta_k \theta}}{(\gamma^{-2} + (\theta_k - \theta)^2)}, \quad (24)$$

where  $\theta_k = \mathbf{k}_\perp/k$ . To compute this integral, we first note that the characteristic angular spread of pseudophotons is determined by the parameter  $\theta_k \approx \gamma^{-1}$ . Consequently, if the condition  $\theta \approx \sigma_a \ll \gamma^{-1}$  is fulfilled, we can ignore the influence of the angular spread of the electron on the angular spread of pseudophotons. This condition can be fulfilled for realistic emittances of electron beams [20]. As a result, in this approximation, the desired integral is given by

$$I = \frac{1}{k_x} \frac{\theta_k}{(\gamma^{-2} + \theta_k^2)} e^{-(xkv)^2 \sigma_a^2 \theta_k^2/4}. \quad (25)$$

As a result, we can find the expression for the coherent part  $\Pi_{\text{coh}}$  of the pseudophotons flux

$$\begin{aligned} \Pi_{\text{coh}} &= \frac{N^2 e_0^2}{2v\pi^2} \int_0^\infty dk_x \int d\theta_k \frac{\theta_k^2 e^{-(xkv)^2 \sigma_a^2 \theta_k^2/2 - \theta_k^2 k^2 \sigma_b^2/2}}{(\gamma^{-2} + \theta_k^2)^2} \\ &\times \left| \frac{1 - e^{iL_b k_x}}{K(1 - e^{id_0 k_x})} \right|^2 e^{-k_x^2 \sigma_c^2/2}. \end{aligned} \quad (26)$$

We first evaluate the integral over the angles

$$J = \int d\theta_k \frac{\theta_k^2}{(\gamma^{-2} + \theta_k^2)^2} e^{-a^2 \theta_k^2}, \quad (27)$$

with  $a^2 = 1/2[(xkv)^2 \sigma_a^2 + k^2 \sigma_b^2]$ . The evaluation of this integral is done in the following way:

$$\begin{aligned} J &= \pi \int_0^\infty du \frac{u}{(\gamma^{-2} + u)^2} e^{-a^2 u} \\ &= \pi \left[ \int_0^\infty du \frac{e^{-a^2 u}}{(\gamma^{-2} + u)} - \int_0^\infty dx \frac{\gamma^{-2} e^{-a^2 u}}{(\gamma^{-2} + u)^2} \right] \\ &= \pi [-e^{a^2 \gamma^{-2}} \text{Ei}(-a^2 \gamma^{-2})(1 + \gamma^{-2} a^2) - 1]. \end{aligned} \quad (28)$$

In this equation,  $\text{Ei}(x)$  is the integral exponential function [21].

Thus, the coherent part of the spectral density of the pseudophotons is represented in the following way ( $k_x = \omega/v$ ;  $K = L_b/d_0$ ):

$$\begin{aligned} n_{\text{coh}}(\omega) &\approx \frac{N^2 e_0^2}{2\pi\omega v^2} \frac{d_0^2}{L_b^2} [-e^{a^2 \gamma^{-2}} \text{Ei}(-a^2 \gamma^{-2})(1 + \gamma^{-2} a^2) - 1] \\ &\times \left| \frac{1 - e^{iL_b \omega/v}}{(1 - e^{id_0 \omega/v})} \right|^2 \exp[-\omega^2 \sigma_c^2/2v^2]. \end{aligned} \quad (29)$$

The spectral density  $n_{\text{coh}}(\omega)$  of coherent pseudophotons has sharp maximums when the frequency  $\omega = 2\pi l/d_0$ ,  $l = 1, 2, \dots$  and the result can be represented in the following form:

$$\begin{aligned} n_{\text{coh}}(\omega) &\approx \frac{N^2 e_0^2}{2\pi\omega v^2} \frac{d_0^2}{L_b^2} [-e^{a^2 \gamma^{-2}} \text{Ei}(-a^2 \gamma^{-2})(1 + \gamma^{-2} a^2) - 1] \\ &\times \sum_{l=1}^K \frac{\sin^2[L_b(\omega - 2\pi l/d_0)/2v]}{\sin^2[d_0(\omega - 2\pi l/d_0)/2v]} e^{-2\pi^2 l^2 \sigma_c^2/d_0^2}. \end{aligned} \quad (30)$$

The factor  $e^{-2\pi^2 \sigma_c^2/d_0^2} \leq 1$  as we supposed that fluctuation of the modulation period defined by the parameter  $\sigma_c < d_0/2\pi$ . These fluctuations are conditioned by the stochasticity inherent to the SASE mechanism.

Let us compare the contributions from the coherent  $n_{\text{coh}}(\omega)$  and incoherent  $n_{\text{sp}}(\omega)$  parts of the spectral densities in Eq. (18). For this, we choose the distribution of the pseudophotons of the LCLS XFEL [20] facility. The typical electron energy is  $E = 6.7$  GeV which corresponds to the electron gamma factor of  $\gamma \approx 13111$ . The parameters  $\sigma_a = 10^{-4}$  and  $\sigma_b = 2 \times 10^{-5}$  cm, parameter  $a^2 \gamma^{-2} \approx 0.2$ . Let the bunch charge be  $Q = 0.2$  nC that corresponds to  $N = 1.2 \times 10^9$  electrons. The duration of the photon pulse

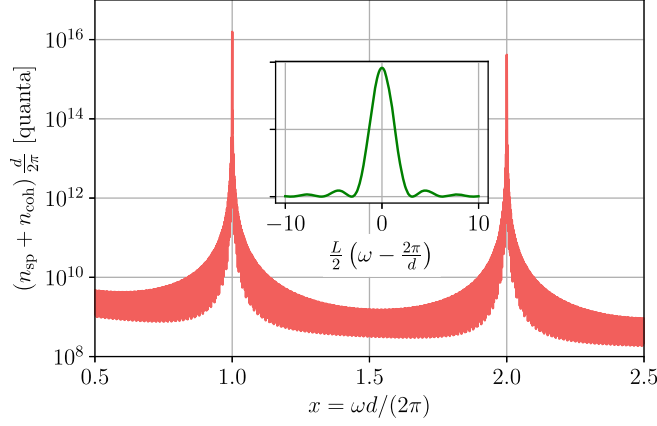


FIG. 3. The incoherent and two harmonics of the coherent pseudophotons spectral densities. The inset demonstrates the zoomed-in peak structure.

we can choose to be 25 fs, which corresponds to the modulated bunch length of  $L_b = 8.3 \times 10^{-5}$  cm and the period of the modulation  $d_0 = 10^{-8}$  cm with the parameter  $\sigma_c = 10^{-9}$  cm. In Fig. 3, we plot the incoherent and two harmonics of the coherent spectral densities of the pseudophotons of a modulated beam with these parameters.

Finally, the typical frequency spread for the XFEL pulse  $\Delta\omega/\omega_0 \approx 10^{-3}$  and the frequency  $\omega_0 = 6.28 \times 10^8$  cm $^{-1}$ . By using a spectral density  $n_{sp}(\omega)$  from Eq. (18), we can evaluate the number of the incoherent pseudophotons in this interval as the integral  $N_{sp} = \int_{\omega_0 - \frac{\Delta\omega}{2}}^{\omega_0 + \frac{\Delta\omega}{2}} n_{sp}(\omega) d\omega \approx n_{sp}(\omega_0) \Delta\omega$ . Thus, we can estimate the number of incoherent photons in the following way:

$$N_{sp} = n_{sp}(\omega_0) \Delta\omega = N \frac{2e_0^2 \Delta\omega}{\pi \omega_0} \ln \frac{E}{\omega_0} = 1.1 \times 10^5, \quad (31)$$

where  $E = m\gamma$  is the energy of the electron.

This number is significantly smaller than the corresponding number of photons emitted by the XFEL pulse [20].

At the same time, the integration of the coherent distribution in the vicinity of the resonant frequency  $\omega_l = 2\pi l/d_0$  can be fulfilled by means of the formula

$$\frac{\sin^2[L_b(\omega - 2\pi l/d_0)/2v]}{\sin^2[d_0(\omega - 2\pi l/d_0)/2v]} \approx 2\pi v \frac{L_b}{d_0^2} \delta(\omega - 2\pi l/d_0), \quad (32)$$

$$L_b \gg d_0.$$

The usage of Eq. (32) in Eq. (30) and integration of  $N_{coh} = \int_{\omega_0 - \frac{\Delta\omega}{2}}^{\omega_0 + \frac{\Delta\omega}{2}} n_{coh}(\omega) d\omega \approx 2\pi v L_b/d_0^2 n_{coh}(\omega_0)$  yield the number of pseudophotons in the first harmonic ( $l = 1$ )

$$N_{coh} = \frac{N^2 e_0^2}{\omega_0 L_b} \left( \ln \frac{1}{a^2 \gamma^{-2}} - C - 1 \right) \approx 5.9 \times 10^{11};$$

$$a^2 \gamma^{-2} \ll 1. \quad (33)$$

Here  $C \approx 0.577$  is the Euler constant. The number  $N_{coh}$  is comparable with the number of photons in the undulator XFEL pulse. In addition, the number of pseudophotons, corresponding to the second harmonic ( $l = 2$ ) is 10 times less.

As was discussed above, the reflection from the crystallographic planes leads to the conversion of the pseudophotons into real photons and corresponds to the SPXE process. The reflection coefficient of the pseudophotons from the crystallographic planes is a function of the pseudophoton frequency. Consequently, the intensity of the SPXE will reach its maximum when the maximum of the spectral density of the pseudophotons coincides with the maximum of their reflection coefficient. If the position of a crystal is chosen as shown in Fig. 2, the pseudophotons whose wave vectors  $\mathbf{k}$  satisfy Bragg's condition with one of the reciprocal lattice vectors  $\mathbf{g}$  of the crystal will have maximal reflection coefficient, i.e.,

$$2\mathbf{k}_0 \cdot \mathbf{g} + g^2 = 0, \quad (34)$$

where  $\mathbf{k}_0 = \omega_0 \mathbf{v}/v$ .

This means that the crystal should be oriented in such a way to the electron bunch that the angle between the electron velocity and the reflection plane equals

$$\theta_B = \arcsin \frac{g}{2\omega_0} \quad (35)$$

and the SPXE pulse will propagate in the direction of  $\mathbf{k}_0 + \mathbf{g}$  under the angle  $2\theta_B$  with respect to the electron velocity, see Fig. 2.

### III. DYNAMIC THEORY OF SPXE

#### A. Electromagnetic field of SPXE

The analysis conducted in the previous sections is valid for the situation when the crystal is thin enough and the diffraction can be investigated in the framework of the kinematic theory. However, the intensity of SPXE reaches its maximum value when the electron propagates the distances in the crystal larger than the corresponding extinction length and consequently, the field created by the particles should be investigated in the framework of the dynamical diffraction theory [15].

This case for regular PXR was investigated in many works and the spectral-angular distribution of the emitted number of PXR quanta was obtained (see [1] and the references therein). The direct generalization of that results for the case of modulated beam leads to the following general expression for the spectral-angular distribution of the emitted number of quanta of SPXE photons:

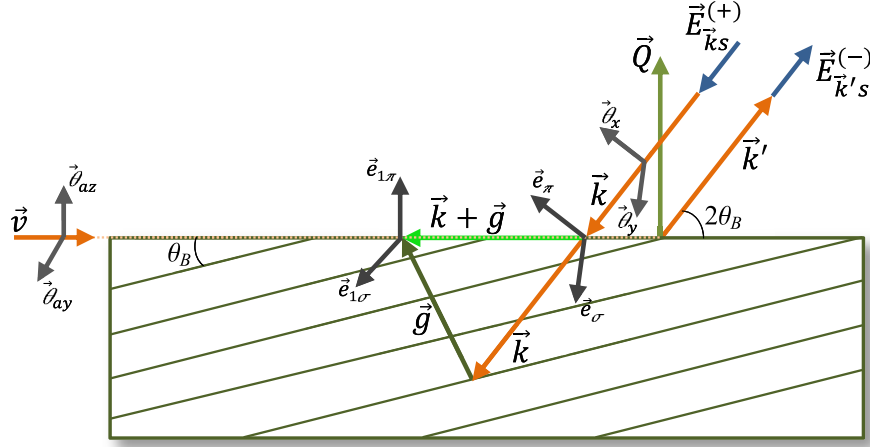


FIG. 4. The geometry for the dynamical diffraction theory of SPXE.

$$\begin{aligned} \frac{\partial^2 N_{n\omega s}}{\partial\omega\partial\Omega} &= \frac{e_0^2\omega}{4\pi^2} \sum_a^N \sum_b^N \int \mathbf{E}_{ks}^{(+)}(\mathbf{r}_a(t), \omega) \mathbf{v}_a e^{i\omega t} dt \\ &\times \int \mathbf{E}_{ks}^{(+)*}(\mathbf{r}_b(t'), \omega) \mathbf{v}_b e^{-i\omega t'} dt', \\ \mathbf{r}_a(t) &= \mathbf{r}_a + \mathbf{v}_a t, \quad \mathbf{k} = -\mathbf{k}', \quad \mathbf{k}' = \omega \mathbf{n}, \end{aligned} \quad (36)$$

where  $\mathbf{k}'$  is the wave vector of the photons emitted in the solid angle  $d\Omega$ ,  $\mathbf{E}_{ks}^{(+)}(\mathbf{r}, \omega)$  is the solution of the Maxwell equations, which describes the diffraction of the plane wave  $\mathbf{e}_s e^{i\mathbf{k}\cdot\mathbf{r}}$  with the polarization  $\mathbf{e}_s$  on the crystal and possesses the asymptotic of the plane wave and an outgoing spherical wave. The use of the wave vector  $\mathbf{k} = -\mathbf{k}'$  and the field  $\mathbf{E}_{ks}^{(+)}$  is related to the fact that for the radiation exited from the crystal, one should exploit the reciprocity theorem of optics [22] that relates the waves with different asymptotics, i.e.,  $\mathbf{E}_{ks}^{(+)} = \mathbf{E}_{-ks}^{(-)*}$ . In addition, it was recently demonstrated that the intensity of the PXR reaches maximal values in the so-called grazing geometry when extremely asymmetric diffraction (EAD) happens. In this geometry, an electromagnetic wave is incident on the crystal under a small angle toward the crystal surface. For this reason, in addition to the diffractive reflection, we need to take into account a specularly reflected wave [15]. For the case of PXR, this means that the bunch of electrons is moving along the crystal surface inside the crystal and the vector  $\mathbf{k}_g = \mathbf{k} + \mathbf{g}$  is antiparallel to the electron velocity, i.e.,  $\mathbf{k}_g \parallel (-\mathbf{v})$  (see Fig. 4).

To find the field created by the particle inside a crystal, we can use the results from Ref. [23] where a two-wave approximation [1,15] of the dynamical diffraction theory was employed according to which the field within the crystal is expressed as

$$\mathbf{E}_{ks}^{(+)}(\mathbf{r}, \omega) = \mathbf{e}_s E_{ks} e^{i\mathbf{k}\cdot\mathbf{r}} + \mathbf{e}_{1s} E_{k_g s} e^{i\mathbf{k}_g \cdot \mathbf{r}}, \quad (37)$$

$$\mathbf{k}_g = \mathbf{k} + \mathbf{g}. \quad (38)$$

Here  $\mathbf{e}_s$  and  $\mathbf{e}_{1s}$  ( $s = 1, 2$ ) are the polarization vectors of the incident and the diffracted waves (Fig. 4). Their amplitudes satisfy the algebraic system of homogeneous equations

$$\begin{aligned} \left( \frac{k^2}{k_0^2} - 1 - \chi_0 \right) E_{ks} - c_s \chi_{-g} E_{k_g s} &= 0, \\ \left( \frac{k_g^2}{k_0^2} - 1 - \chi_0 \right) E_{k_g s} - c_s \chi_g E_{ks} &= 0, \end{aligned} \quad (39)$$

where  $k_0 = \omega$ ,  $\chi_0$ , and  $\chi_g$  are the Fourier components of the crystal susceptibility  $\chi(\mathbf{r})$

$$\chi(\mathbf{r}) = \sum_g \chi_g e^{i\mathbf{g}\cdot\mathbf{r}}. \quad (40)$$

The coefficient  $c_s = 1$  for the  $\sigma$  polarization ( $s = 1$ ) and  $c_s = \cos 2\theta_B$  for the  $\pi$  polarization ( $s = 2$ ) of the incident and diffracted waves, respectively. In addition, we note that the waves of different polarizations propagate independently if we neglect terms of the order of  $\sim |\chi_0|^2$  in the Maxwell equations [14,15,24].

The field amplitudes in vacuum and in crystal should satisfy the boundary conditions on the crystal-vacuum interface such that the total field intensity is continuous. Additionally, one needs to take into account in vacuum not only an incident wave but also a specularly reflected diffracted wave  $\mathbf{E}_{k_g s}^{(sp)} = \mathbf{e}_{1s} E_{k_g s}^{(sp)} \exp[i(\mathbf{k}_{\parallel} + \mathbf{g}_{\parallel}) \cdot \mathbf{r} + ik'_{gz} z]$ ,  $k'_{gz} = \sqrt{k_0^2 - (\mathbf{k}_{\parallel} + \mathbf{g}_{\parallel})^2}$ , where  $\mathbf{k}_{\parallel}$  and  $\mathbf{g}_{\parallel}$  are the projections of the vectors on the crystal surface. As a result, the following expressions for the field inside and outside the crystal were found [23]

$$\mathbf{E}_{ks}^{(+)} = \mathbf{e}_s e^{i\mathbf{k}\cdot\mathbf{r}} + \mathbf{e}_{1s} E_s^{(sp)} e^{i(\mathbf{k}_{\parallel} + \mathbf{g}_{\parallel}) \cdot \mathbf{r}} e^{ik'_{gz} z}, \quad z > 0, \quad (41)$$

$$\mathbf{E}_{ks}^{(+)} = e^{i\mathbf{k}\cdot\mathbf{r}} \sum_{\mu=1,2} e^{-ik_0 z \epsilon_{\mu s}} (\mathbf{e}_s E_{\mu s} + \mathbf{e}_{1s} E_{g\mu s} e^{ig\cdot\mathbf{r}}), \quad z < 0, \quad (42)$$

where the  $x$  axis is directed along the propagation direction of the electron bunch and the  $z$  axis is directed perpendicular to the crystal surface. The coordinate  $x$  is changing in the limits  $0 < x < L$ , with  $L$  being the crystal length, Fig. 2, and the point  $z = 0$  denotes the crystal surface with  $z < 0$  as the crystal and  $z > 0$  as vacuum. The quantities  $\epsilon_{\mu s}$  define the wave vector inside the crystal and are determined from the condition that the system of homogeneous equations (39) has a nontrivial solution. The  $\mathbf{Q}$  is normal to the crystal surface. The field amplitudes  $E_s^{(sp)}$ ,  $E_{\mu s}$ , and  $E_{g\mu s}$  are found from the boundary conditions. According to the boundary conditions, the in-plane component  $k_{\parallel}$  of the wave vector is conserved. Finally, it was found that the main contribution to the number of emitted photons is given by the amplitude  $E_{g1s}$  which reads

$$E_{g1s} = \frac{c_s \chi g}{\alpha_B + \chi_0}, \quad (43)$$

$$\alpha_B = \frac{(\mathbf{k} + \mathbf{g})^2 - k_0^2}{k_0^2}. \quad (44)$$

Here the coefficient  $\alpha_B$  defines the deviation from the Bragg's condition.

### B. The radiation spectral-angular distribution

As in the case of kinematic theory, we can split the total intensity in Eq. (36) into coherent and incoherent parts. The latter part corresponds to the situation when in the double sum we select only the terms with identical indices, i.e.,  $a = b$ . This contribution is proportional to the number of electrons in the bunch  $N$  and corresponds to the spontaneous parametric x-ray radiation (PXR):

$$\frac{\partial^2 N_{nos}^{sp}}{\partial \omega \partial \Omega} = N \frac{e_0^2 \omega}{4\pi^2} \left| \int \mathbf{E}_{ks}^{(+)}(\mathbf{r}(t), \omega) \mathbf{v} e^{i\omega t} dt \right|^2, \quad (45)$$

$$\mathbf{r}(t) = \mathbf{r}_0 + \mathbf{v}t.$$

The integral over the electron trajectory was computed in Ref. [23], which yields the

$$\frac{\partial^2 N_{no}^{sp}}{\partial \theta_x \partial \theta_y} = N \frac{e_0^2}{4\pi \hbar c} \frac{[(\theta_y - \theta_{ay})^2 + (\theta_x - \theta_{az})^2 \cos^2 2\theta_B] |\chi g|^2}{[\gamma^{-2} + (\theta_y - \theta_{ay})^2 + (\theta_x - \theta_{az})^2 - \chi_0']^2} \times \frac{(1 - e^{-Lk_0 \chi_0' |\theta_{az}|})}{\chi_0'' |\theta_{az}|} e^{-\chi_0' k_0 |z_0|}. \quad (46)$$

In this equation, the angles  $\theta_a, \theta$  are the angular variables of the electron and the emitted photon correspondingly (Fig. 4). They define small deviations of the electron

velocity and the photon wave vector from the ideal values. Therefore, we can introduce the following quantities:

$$\begin{aligned} \mathbf{v}_a &= v \left( 1 - \frac{\theta_a^2}{2} \right) \mathbf{e}_x + \boldsymbol{\theta}_a; & (\mathbf{e}_x \boldsymbol{\theta}_a) &= 0; \\ \mathbf{k} &= \mathbf{k}_0 \left( 1 - \frac{\theta_a^2}{2} \right) + k_0 \boldsymbol{\theta}; & (\mathbf{k}_0 \boldsymbol{\theta}) &= 0; \\ \omega + (\mathbf{k}_0 + \mathbf{g}) \cdot \mathbf{v} &= 0; & 2(\mathbf{k}_0 \mathbf{g}) + g^2 &= 0. \end{aligned} \quad (47)$$

The integral over  $\boldsymbol{\theta}$  and averaging over the electron angles were computed in Ref. [23]. For example, for Si crystal, the characteristic value of the photon number for PXR in EAD geometry is

$$N_{\text{PXR}}^{sp} \approx 2.2 \times 10^{-5} \times N \approx 0.3 \times 10^5, \quad (48)$$

for the bunch with charge  $Q_0 = 0.2$  nC, i.e.,  $N = 1.3 \times 10^9$ .

A detailed comparison of the theoretical and experimental results for the spontaneous PXR in the EAD geometry has been considered in the paper [25].

This value is comparable with the value of spontaneous pseudophotons defined by Eq. (31) that is the crystal is working as the reflective mirror for this interval of the pseudophoton spectrum.

Now let us come back to compute the coherent part of the distribution. We also perform the same substitution from the summation over the discrete index by the integration over the electron distribution. In this case, the calculation is reduced to the calculation of the following averaging with the distribution functions of the bunch:

$$\frac{\partial^2 N_{n,os}^{\text{coh}}}{\partial \omega \partial \Omega} = N^2 \frac{e_0^2 \omega}{4\pi^2} |F_s(\mathbf{k})|^2 \quad (49)$$

$$F_s(\mathbf{k}) = \frac{1}{N} \int \left\langle \sum_a^N \mathbf{E}_{ks}^{(+)}(\mathbf{r}_a(t), \omega) \mathbf{v}_a e^{i\omega t} \right\rangle dt, \quad (50)$$

$$\mathbf{v}_a = v \left( 1 - \frac{\theta_a^2}{2} \right) + v \boldsymbol{\theta}_a, \quad \mathbf{v} \cdot \boldsymbol{\theta}_a = 0. \quad (51)$$

Here we considered that the electron velocity has deviations from the  $x$  axis and these deviations are described by the  $\boldsymbol{\theta}_a$ . The vector  $\mathbf{v}$  is the mean velocity of the electron bunch and is directed along the  $x$  axis (Fig. 4).

As was already discussed, the SPXE emission is related to the motion of the bunch of electrons in a thin layer inside the crystal parallel to the crystal-vacuum interface. In this case, the electron velocity is perpendicular to the normal  $\mathbf{Q}$  to the crystal surface, i.e.,  $\mathbf{v} \cdot \mathbf{Q} = 0$ . We are interested in the diffracted wave, that is the wave which is propagating in the direction  $\mathbf{k}_g = \mathbf{k} + \mathbf{g}$ . Consequently, the main contribution is given by the  $E_{g1s}$  amplitude. Therefore, the field which is entering into the desired averaging reads

$$\begin{aligned} E_{ks}^{(+)}(\mathbf{r}_a(t), \omega) e^{i\omega t} &= \mathbf{e}_{1s} E_{g1s} \exp\{i(\omega + \mathbf{k}_g \cdot \mathbf{v} - \omega \mathbf{Q} \cdot \boldsymbol{\theta}_{\epsilon_{1s}})t \\ &\quad + i\mathbf{v} \mathbf{k}_g \cdot \boldsymbol{\theta}_a t - i\mathbf{k}_g \cdot \mathbf{v} t \theta_a^2 / 2 \\ &\quad + i\mathbf{k}_g \cdot \mathbf{r}_a - i k_0 \mathbf{r}_a \cdot \mathbf{Q} \epsilon_{1s}\}. \end{aligned} \quad (52)$$

According to the results of Ref. [23], the SPXE peak is located near the direction defined by the conditions Bragg's diffraction condition

$$\alpha_B = \frac{(\mathbf{k} + \mathbf{g})^2 - k_0^2}{k_0^2} = 0. \quad (53)$$

The Cherenkov radiation condition

$$(\mathbf{k} + \mathbf{g}) \cdot \mathbf{v} = -k_0 = -\omega. \quad (54)$$

The condition that extremely asymmetric diffraction happens, i.e., the diffracted wave is propagating in the direction of  $\mathbf{k}_g$ , which lies in the crystal plane defined by the normal to the crystal surface  $\mathbf{Q}$

$$(\mathbf{k} + \mathbf{g}) \cdot \mathbf{Q} = 0. \quad (55)$$

Taking into account these considerations, we can represent the vector  $\mathbf{k}_g$  in the following way:

$$\mathbf{k}_g = -\frac{\omega}{v^2} \mathbf{v} \left(1 - \frac{\theta^2}{2}\right) + \omega \boldsymbol{\theta}, \quad \boldsymbol{\theta} \cdot \mathbf{v} = 0. \quad (56)$$

With this, the form factor of the bunch is defined by the following integral with the accuracy  $\sim \theta^3$ :

$$\begin{aligned} F_s(\omega, \boldsymbol{\theta}) &= \int_0^L dt \mathbf{e}_{1s} \cdot \mathbf{v} \frac{c_s \chi_g}{\alpha_B + \chi_0} e^{i(\omega + \mathbf{k}_g \cdot \mathbf{v} - \omega \mathbf{Q} \cdot \boldsymbol{\theta}_{\epsilon_{1s}})t} J, \\ J &= \int d\mathbf{r}_a d\boldsymbol{\theta}_a f(\mathbf{r}_a) \rho(\boldsymbol{\theta}_a) \exp\left\{i\omega \boldsymbol{\theta} \boldsymbol{\theta}_a t + \frac{i\omega t \theta_a^2}{2} \right. \\ &\quad \left. + i\omega(-x_a + \boldsymbol{\theta} \mathbf{r}_a)\right\} \end{aligned} \quad (57)$$

The evaluation of the integral  $J$  over electron angle and coordinates with the Gaussian distribution [Eqs. (20) and (21)] yields

$$\begin{aligned} J &= \exp\left\{-\frac{\omega^2 t^2 \theta^2 \sigma_a^2}{4(1 + i\omega t \sigma_a^2)} - \frac{\omega^2 \theta^2 \sigma_b^2}{4} - \frac{\omega^2 \sigma_c^2}{4}\right\} \\ &\quad \times \frac{1 - e^{iL_b \omega}}{K(1 - e^{i d_0 \omega})}. \end{aligned} \quad (58)$$

The maxima of  $J$  as a function of  $\omega$  are located on the frequencies  $\omega$  of the radiation, which is proportional to the frequencies of the modulation of the electron beam, i.e.,  $\omega = \omega_0 n$ , where  $\omega_0 = 2\pi/d_0$ . In addition, it follows from Eq. (58) that the major contribution to the coherent pulse of SPXE comes from the part of an electron trajectory and

scattering angles for which the following conditions are fulfilled:

$$\omega t \theta \sigma_a < 1, \quad (59)$$

$$\omega \theta \sigma_b < 1. \quad (60)$$

Since the angular spread  $\sigma_a$  of ultrarelativistic electrons in the beam of XFEL is significantly smaller than the angular spread of PXR photons, for which  $\theta \simeq \sqrt{|\chi'_0|}$  [1], the terms  $\omega t \sigma_a^2$  in Eq. (58) can be neglected. In this case, one can perform the integration over time  $t$  in an analytical form. This gives

$$\begin{aligned} F_s(\omega, \boldsymbol{\theta}) &= \frac{c_s (\mathbf{e}_{1s} \cdot \mathbf{v}) \chi_g}{\alpha_B + \chi_0} \frac{1 - e^{iL_b \omega}}{K(1 - e^{i d_0 \omega})} \\ &\quad \times e^{-\frac{\omega^2 \sigma_c^2}{4} - \frac{\omega^2 \theta^2 \sigma_b^2}{4}} e^{\frac{q_s^2}{\delta^2} \frac{\sqrt{\pi}}{\delta}} \\ &\quad \times \left[ \Phi\left(\frac{L\delta}{2} + i \frac{q_s}{\delta}\right) - \Phi\left(-i \frac{q_s}{\delta}\right) \right], \end{aligned} \quad (61)$$

where  $\Phi(x) = \frac{2}{\sqrt{\pi}} \int_x^\infty e^{-y^2} dy$  is the complementary error function,  $\delta = \omega \theta \sigma_a$ ,  $q_s = \omega + \mathbf{k}_g \cdot \mathbf{v} - \omega \mathbf{Q} \cdot \boldsymbol{\theta}_{\epsilon_{1s}}$ .

According to Ref. [23] when Eqs. (55) and (54) and the additional condition  $\theta \gg \sigma_a$  are satisfied, the quantity  $\alpha_B$  is expressed through the angular variables of a photon as

$$\alpha_B \approx -(\gamma^{-2} + \theta^2). \quad (62)$$

As a result, we obtain an expression for the spectral-angular distribution of photons in the coherent part of the SPXE pulse, which for the first harmonic  $u = \omega - 2\pi/d_0$

$$\begin{aligned} \frac{\partial^2 N_{n\omega s}^{\text{coh}}}{\partial \omega \partial \Omega} &= N^2 \frac{e_0^2 \omega}{4\pi^2} \frac{c_s^2 (\mathbf{e}_{1s} \cdot \mathbf{v})^2 |\chi_g|^2}{(\gamma^{-2} + \theta^2 - \chi'_0)^2} \frac{\sin^2 L_b u / 2}{K^2 \sin^2 d_0 u / 2} \\ &\quad \times \exp\left\{-\frac{2\pi^2 \sigma_c^2}{d^2} - \frac{\omega^2 \theta^2 \sigma_b^2}{2} - 2 \frac{q_s^2}{\delta^2}\right\} \\ &\quad \times \frac{\pi}{\delta^2} \left| \Phi\left(\frac{L\delta}{2} - i \frac{q_s}{\delta}\right) - \Phi\left(-i \frac{q_s}{\delta}\right) \right|^2. \end{aligned} \quad (63)$$

### C. Characteristics of the SPXE pulse

Now we compute the total number of quanta in the coherent part of SPXE. For this, we need to integrate the spectral-angular distribution (63) over the angles and frequencies. To compute the integral over the frequencies, we make use of the following relation:

$$\frac{\sin^2 L_b u / 2}{K^2 \sin^2 d_0 u / 2} \approx 2\pi \frac{1}{L_b} \delta(\omega - \omega_0), \quad (64)$$

which is valid when  $K = L_b/d_0 \gg 1$ . Here  $\omega_0 = 2\pi/d_0$ . Consequently, the integration over the frequency becomes trivial

$$\begin{aligned} \frac{\partial^2 N_{n\omega s}^{\text{coh}}}{\partial \Omega} &= N^2 \frac{e_0^2 \omega_0}{2L_b} \frac{c_s^2 (\mathbf{e}_{1s} \cdot \mathbf{v})^2 |\chi_g|^2}{(\gamma^{-2} + \theta^2 - \chi_0')^2} \\ &\times \exp \left\{ -\frac{2\pi^2 \sigma_c^2}{d^2} - \frac{\omega_0^2 \theta^2 \sigma_b^2}{2} - 2\frac{q_s^2}{\delta^2} \right\} \\ &\times \frac{1}{\delta^2} \left| \Phi \left( \frac{L\delta}{2} - i\frac{q_s}{\delta} \right) - \Phi \left( -i\frac{q_s}{\delta} \right) \right|^2 \Big|_{\omega=\omega_0}. \end{aligned} \quad (65)$$

When an electron bunch moves in the crystal, its angular divergence increases due to the multiple scattering on the atoms of the crystal. As was demonstrated in Ref. [26] for PXR from ultrarelativistic electrons, it can be taken into account with the help of the substitution

$$\begin{aligned} \gamma^{-2} &\Rightarrow \tilde{\gamma}^{-2} = \gamma^{-2} + \theta_s^2, \\ \theta_s^2 &= \left( \frac{E_s}{E} \right)^2 \frac{L}{L_R}, \end{aligned} \quad (66)$$

where  $L_R$  is the radiation length [17] and  $E_s \approx 21$  MeV.

Let us now investigate this expression for the case of an ideal electron beam for which the following conditions are fulfilled:

$$\frac{2\pi^2 \sigma_c^2}{d_0^2} < 1, \quad (67)$$

$$\omega^2 \theta^2 \sigma_b^2 \approx \omega^2 |\tilde{\gamma}^{-2} - \chi_0'| \sigma_b^2, \quad (68)$$

$$\delta^2 L^2 = (\omega \theta \sigma_a)^2 L^2 \approx (\omega L \sigma_a)^2 |\tilde{\gamma}^{-2} - \chi_0'| < 1. \quad (69)$$

The first condition means that the fluctuations of the modulation period are rather small. The analogous condition should be also fulfilled for the formation of the XFEL pulse based on the undulator radiation [10,19]. As well as for XFEL pulses, the stochasticity inherent to the SASE mechanism gives rise to chaotic SPXE pulses with strong fluctuations in their amplitudes and phases which vary from shot to shot.

The meaning of the remaining ones is that the relative transverse width and the angular spread of the particles in the bunch are less than the angular divergence of the photons in the PXR pulse [23]. These conditions restrict the exploited electron beams only to the high quality ones with a low emittance. For example, if we consider electrons with the energy of 6.7 GeV, propagating through a silicon crystal of a thickness  $L = 1$  cm and generating photons with the energy of 10 KeV ( $|\chi_0'| \approx 10^{-5}$ ), then we get the following estimation for the beam emittance (under these conditions  $\tilde{\gamma}^{-2} < |\chi_0'|$  and the restrictions on the emittance are weakly dependent on the electron energy):

$$\begin{aligned} \sigma_b^2 &< 10^{-11} \text{ cm}, \quad \sigma_a^2 < 10^{-9} \text{ rad}, \\ \epsilon &= \sigma_b \sigma_a < 10^{-10} \text{ cm} \times \text{rad}, \end{aligned} \quad (70)$$

which is sizable for the LCLS facility.

Under the assumptions of Eqs. (67)–(69), we can further simplify the expression for the number of emitted photons. For this, we notice that for large  $x$ , the complementary error function can be replaced by its asymptotic representation  $\Phi(x) \approx 1/\sqrt{\pi} e^{-x^2}/x$  and Eq. (65) is further simplified

$$\begin{aligned} \frac{\partial N_{ns}^{\text{coh}}}{\partial \Omega} &= N^2 \frac{e_0^2 \omega_0}{2L_b} \frac{c_s^2 (\mathbf{e}_{1s} \cdot \mathbf{v})^2 |\chi_g|^2}{(\tilde{\gamma}^{-2} + \theta^2 - \chi_0')^2} \\ &\times \frac{1}{\pi} \left| \frac{1 - e^{iq_s L}}{q_s} \right|^2. \end{aligned} \quad (71)$$

Now taking into account that when  $\omega_0 L \gg 1$ , we replace [1]

$$\frac{1}{\pi} \left| \frac{1 - e^{iq_s L}}{q_s} \right|^2 = \frac{4 \sin^2 L q_s / 2}{\pi q_s^2} \approx 2L \delta(q_s) \quad (72)$$

and integrate over the angle  $\theta_x$  in the plane, defined by the vectors  $\mathbf{v}$  and  $\mathbf{g}$  with the value

$$\begin{aligned} q_s &= \omega_0 + (\mathbf{k}_g \cdot \mathbf{v}) - \omega_0 \epsilon_{1s} \theta_x \\ &\approx \omega_0 + (\mathbf{k}_0 + \mathbf{g}) \cdot \mathbf{v} - \omega_0 \theta_x \sin 2\theta_B = 0; \\ \theta_x &= \frac{(\mathbf{k}_0 + \mathbf{g}) \cdot \mathbf{v}}{\omega_0 \sin 2\theta_B} = 0. \end{aligned} \quad (73)$$

As a result, the photons are emitted with the polarization proportional to  $\theta_y$  and directed along the vector  $\mathbf{v} \times \mathbf{g}$  (Fig. 4). Thus, we get

$$\frac{\partial N_{\theta_y}^{\text{coh}}}{\partial \theta_y} = N^2 \frac{e_0^2 |\chi_g|^2 \theta_y^2}{(\tilde{\gamma}^{-2} + \theta_y^2 - \chi_0')^2} \frac{L}{L_b \sin 2\theta_B}. \quad (74)$$

We pay attention here to the fact that the SPXE pulse has an asymmetric angular distribution in comparison with the XFEL pulse. According to Eq. (74), the angular widths of the SPXE pulse in the directions of  $x$  and  $y$  axes are determined by the following:

$$\begin{aligned} \Delta \theta_x &\approx \Delta \omega / \omega \approx 1/K \sim 10^{-4}; \\ \Delta \theta_y &\approx \sqrt{\tilde{\gamma}^{-2} - \chi_0'} \sim 10^{-3}. \end{aligned} \quad (75)$$

Finally, after the integration over the remaining angle  $\theta_y$ , one obtains the total number of the SPXE photons:

$$N_{\text{SPXE}} = N^2 \frac{e_0^2 |\chi_g|^2 \pi}{2\sqrt{\tilde{\gamma}^{-2} - \chi_0'}} \frac{L}{L_b \sin 2\theta_B}. \quad (76)$$

This result provides a clear qualitative interpretation if we relate  $N_{\text{SPXE}}$  with the number of the coherent

pseudophotons  $N_{\text{coh}}$ , defined by Eq. (33). With logarithmic accuracy, one obtains

$$N_{\text{SPXE}} \approx \frac{\pi}{2 \sin 2\theta_B} \frac{|\chi_g|^2 \omega_0 L}{\sqrt{\tilde{\gamma}^{-2} - \chi'_0}} N_{\text{coh}}. \quad (77)$$

The reflection coefficient  $R$  of x-ray radiation on the crystallographic planes is defined by the equation [24]

$$R \approx |\chi_g|^2 (\omega_0 L)^2$$

Here the Bragg's condition is fulfilled.

If one takes into account the ratio of the angular width of the Bragg's peak  $\Delta\theta_B \approx (\omega_0 L)^{-1}$  to the angular spread of the pseudophotons  $\Delta\theta_{\text{ps}} \approx \sqrt{\tilde{\gamma}^{-2} - \chi'_0}$ , then Eq. (77) takes the following form:

$$N_{\text{SPXE}} \approx \frac{\pi}{2 \sin 2\theta_B} R \frac{\Delta\theta_B}{\Delta\theta_{\text{ps}}} N_{\text{coh}}. \quad (78)$$

This relation demonstrates that the SPXE emerges as a result of the reflection of coherent pseudophotons from the crystallographic planes. The frequencies of these pseudophotons are located near the frequency of the resonance  $\omega_0 = 2\pi/d_0$ .

The real photons are emitted under the large angle  $2\theta_B$  to the electron velocity. Thus, by choosing the orientation of the crystal, the photons can be directed in any desired location. This allows one to obtain additional experimental windows in the XFEL experiments.

In order to get a quantitative estimation, we consider that an electron bunch has a charge of 0.2 nC and the length  $L_b = 8.3 \times 10^{-5}$  cm.

For the crystal parameters, we will employ the values taken from the x-ray database [27] for the SPXE radiation generated in a Si crystal by the reflection (400) and  $\theta_B = \pi/4$

$$\begin{aligned} \hbar\omega_B &= 6.45 \text{ keV}; & k_0 &= 3.27 \times 10^8 \text{ cm}^{-1}; \\ E &= 6.7 \text{ GeV}; & |\chi_g| &= 0.12 \times 10^{-4}; & \chi'_0 &= -0.24 \times 10^{-5}; \\ L &= 1.0 \text{ cm}; & \tilde{\gamma}^{-2} &= 7.5 \times 10^{-7} \end{aligned} \quad (79)$$

The crystal surface is defined by the plane  $\langle 110 \rangle$ . The photons will be emitted under the angle  $\pi/2$  to the electron velocity.

As a result, we obtain the number of photons in the coherent part of SPXE

$$N_{\text{SPXE}} \approx 5.7 \times 10^{12} \text{ quanta} \quad (80)$$

with the angular spread  $\delta\theta$  and spectral width  $\Delta\omega/\omega$  of the order  $\sqrt{\tilde{\gamma}^{-2} - \chi'_0} \approx 0.51 \times 10^{-3}$ , which are comparable with the XFEL values.

Also, we pay attention to the fact that according to Eq. (2), the higher harmonics of SPXE will be generated (for the harmonic  $n$ , the condition  $\pi n \sigma_c < d$  should be satisfied). Moreover, they all will be directed under different angles with respect to the electron velocity. For example, for the same crystal parameters, the photons with energy  $\hbar\omega_B = 12.9$  keV will be generated under the angle  $40.5^\circ$  to the electron velocity. This allows one to obtain also intensive pulses of the harder x rays without the need to change the electron energy which is not possible for XFEL.

It is important to notice that the heating of the crystal and the losses of the energy by the electron beam inside the crystal in the SPXE are governed by the same processes as in the case of PXR, which were recently analyzed in the work [8].

#### IV. CONCLUSIONS

In the present paper, a new application of the modulated electron bunches is considered. It is supposed that such bunches are formed in the XFEL undulator due to the SASE mechanism and it is shown that the spectrum of the self-electromagnetic field (pseudophoton spectrum) of such bunches essentially transforms and includes intense peaks at the frequencies proportional to the modulation frequency. When such a bunch goes through the crystal disposed at the undulator exit, the superradiant parametric x-ray emission (SPXE) is generated. Electrons move in the thin layer along the crystal surface and generate an x-ray pulse that is emitted at a large angle to the direction of the electron velocity. The intensity of this pulse is proportional to the square of the number of electrons in the bunch and its characteristics are comparable with the parameter of the main XFEL pulse, which is directed along the electron velocity. SPXE pulses can be used for the creation of additional windows for XFEL. Moreover, the higher harmonics of SPXE can be used for the generation of the pulses of harder x rays and they do not require changing the energy of the electron bunch.

#### ACKNOWLEDGMENTS

The authors are grateful to Professor A. P. Ulyanekov for valuable discussions and support during the project.

- 
- [1] Vladimir G. Baryshevsky, Ilya D. Feranchuk, and Alexander P. Ulyanekov, *Parametric X-Ray Radiation in Crystals: Theory, Experiment and Applications*, Springer Tracts in Modern Physics (Springer, New York, 2006).
  - [2] J. Hyun, M. Satoh, M. Yoshida, T. Sakai, Y. Hayakawa, T. Tanaka, K. Hayakawa, I. Sato, and K. Endo, Compact and intense parametric x-ray radiation source based on a linear accelerator with cryogenic accelerating and decelerating

- copper structures, *Phys. Rev. Accel. Beams* **21**, 014701 (2018).
- [3] Y. Hayakawa, I. Sato, K. Hayakawa, T. Tanaka, A. Mori, T. Kuwada, T. Sakai, K. Nogami, K. Nakao, and T. Sakae, Status of the parametric x-ray generator at LEBRA, Nihon University, *Nucl. Instrum. Methods Phys. Res., Sect. B* **252**, 102 (2006).
- [4] W. Lauth, H. Backe, O. Kettig, P. Kunz, A. Sharafutdinov, and T. Weber, Coherent x-rays at MAMI, *Eur. Phys. J. A* **28**, 185 (2006).
- [5] K. H. Brenzinger, C. Herberg, B. Limburg, H. Backe, S. Dambach, H. Euteneuer, F. Hagenbuck, H. Hartmann, K. Johann, K. H. Kaiser, O. Kettig, G. Knies, G. Kube, W. Lauth, H. Schöpe, and Th. Walcher, Investigation of the production mechanism of parametric x-ray radiation, *Z. Phys. A* **358**, 107 (1997).
- [6] K.-H. Brenzinger, B. Limburg, H. Backe, S. Dambach, H. Euteneuer, F. Hagenbuck, C. Herberg, K. H. Kaiser, O. Kettig, G. Kube, W. Lauth, H. Schöpe, and Th. Walcher, How Narrow is the Linewidth of Parametric X-ray Radiation?, *Phys. Rev. Lett.* **79**, 2462 (1997).
- [7] P. Rullhusen, X. Artru, and P. Dhez, *Novel Radiation Sources Using Relativistic Electrons: From Infrared to X-rays*, Series in Mathematical Biology and Medicine (World Scientific, Singapore, 1998).
- [8] O. D. Skoromnik, I. D. Feranchuk, J. Evers, and C. H. Keitel, Parametric Mössbauer radiation source, *Phys. Rev. Accel. Beams* **25**, 040704 (2022).
- [9] V. G. Baryshevsky and I. D. Feranchuk, Parametric beam instability of relativistic charged particles in a crystal, *Phys. Lett.* **102A**, 141 (1984).
- [10] A. Gover, R. Ianculescu, A. Friedman, C. Emma, N. Sudar, P. Musumeci, and C. Pellegrini, Superradiant and stimulated-superradiant emission of bunched electron beams, *Rev. Mod. Phys.* **91**, 035003 (2019).
- [11] Here and through the manuscript, we use natural units with  $\hbar = c = 1$ .
- [12] W. S. Graves, K. K. Berggren, S. Carbajo, R. Hobbs, K. Hong, W. Huang, F. Kärtner, P. Keathley, D. Moncton, E. Nanni *et al.*, Compact XFEL light source, in *Proceedings of the 35th International Free-Electron Laser Conference, New York, NY* (JACoW, Geneva, Switzerland, 2013).
- [13] Xinlu Xu, Fei Li, Frank S. Tsung, Kyle Miller, Vitaly Yakimenko, Mark J. Hogan, Chan Joshi, and Warren B. Mori, Generation of ultrahigh-brightness pre-bunched beams from a plasma cathode for x-ray free-electron lasers, *Nat. Commun.* **13**, 1 (2022).
- [14] O. D. Skoromnik, V. G. Baryshevsky, A. P. Ulyanenko, and I. D. Feranchuk, Radical increase of the parametric x-ray intensity under condition of extremely asymmetric diffraction, *Nucl. Instrum. Methods Phys. Res., Sect. B* **412**, 86 (2017).
- [15] A. Authier, *Dynamical Theory of X-ray Diffraction* (Oxford University Press, Oxford, New York, 2001).
- [16] A. I. Akhiezer and V. B. Berestetskii, *Quantum Electrodynamics*, Interscience Monographs and Texts in Physics and Astronomy (Interscience, New York, 1965).
- [17] Mikhail Leonovich Ter-Mikaelian, *High-Energy Electromagnetic Processes in Condensed Media* (John Wiley & Sons, New York, 1972), Vol. 29.
- [18] L. D. Landau and E. M. Lifshitz, *The Classical Theory of Fields*, Course of Theoretical Physics (Butterworth-Heinemann, Washington, DC, 1975).
- [19] Zhirong Huang and Kwang-Je Kim, Review of x-ray free-electron laser theory, *Phys. Rev. ST Accel. Beams* **10**, 034801 (2007).
- [20] J. Feldhaus, M. Krikunova, M. Meyer, Th. Möller, R. Moshhammer, A. Rudenko, Th. Tschentscher, and J. Ullrich, AMO science at the FLASH and European XFEL free-electron laser facilities, *J. Phys. B* **46**, 164002 (2013).
- [21] Emde Janke and F. E. Losch, *Tafeln Hoherer Funktionen* (Verlagsgesellschaft, Stuttgart, 1960).
- [22] M. Born and E. Wolf, *Principles of Optics: Electromagnetic Theory of Propagation, Interference and Diffraction of Light* (Elsevier Science, New York, 2013).
- [23] O. D. Skoromnik, I. D. Feranchuk, and D. V. Lu, Parametric x-ray radiation in the Smith-Purcell geometry for non-destructive beam diagnostics, *Nucl. Instrum. Methods Phys. Res., Sect. B* **444**, 125 (2019).
- [24] A. Benediktovich, I. Feranchuk, and A. Ulyanenko, *Theoretical Concepts of X-Ray Nanoscale Analysis: Theory and Applications*, Springer Series in Materials Science (Springer, Berlin, Heidelberg, 2013).
- [25] V. G. Baryshevsky, I. D. Feranchuk, A. O. Grubich, and A. V. Ivashin, Theoretical interpretation of parametric x-ray spectra, *Nucl. Instrum. Methods Phys. Res., Sect. A* **249**, 306 (1986).
- [26] I. Feranchuk and A. Ivashin, Theoretical investigation of the parametric x-ray features, *J. Phys. France* **46**, 1981 (1985).
- [27] S. A. Stepanov, X-ray dynamical diffraction web server, <http://x-server.gmca.aps.anl.gov/>.